

Experimental modelling of deformation around rigid particles in pure shear. The impact of layer anisotropy

Modelización experimental de la deformación alrededor de partículas rígidas en cizalla pura. El impacto de la anisotropía de capas

Ramon Pascual, Elena Druguet and Jordi Carreras

Departament de Geologia, Universitat Autònoma de Barcelona, 08193 Bellaterra (Barcelona).

ramon_04@hotmail.es, elena.druguet@uab.cat, jordi.carreras@uab.cat

ABSTRACT

This work focuses on how the rotation of rigid particles is influenced by preexisting planar anisotropy of the bounding media during deformation. Three experiments were conducted at the UAB Laboratory of Deformation using the apparatus BCN-Stage. The models were made with analogue materials (plasticine as the matrix and paraffin as rigid inclusions) and were deformed by pure shear at constant bulk strain rate and temperature. In the first experiment, in which the matrix consisted of homogeneous plasticine, rotation of the rigid particles agreed with that of previous theoretical and experimental models. In the other two experiments, the rigid paraffin particles were embedded in multilayers of plasticine subjected to folding. The multilayers in both experiments had opposite initial vergences with respect to the kinematic axes. In these two cases, rigid inclusions rotate antithetically with respect to the layers that are being folded, regardless of their initial orientation, indicating the strong influence of layer anisotropy and its orientation on the rotation of rigid objects. The experiments can be correlated with natural field examples at multiple scales, from single crystals in metamorphic rocks to plutons

Key-words: Analogue modelling, deformation partitioning, folding, multilayer, rigid particle rotation.

Geogaceta, 60 (2016), 39-42
ISSN (versión impresa): 0213-683X
ISSN (Internet): 2173-6545

Introduction

Rigid body rotation (porphyroblasts/clasts) in ductile media is a complex issue that has generated a debate in the structural geology field during the last four decades. Such an interest is due to the potential use of these structures as kinematic indicators of deformed terrains (Vernon, 1978; Bell, 1985; Passchier and Simpson, 1986; Johnson, 1999; Passchier and Trouw, 2005). The subject has been addressed from multiple perspectives, including the geometry of field structures and microstructures

(Schoneveld, 1977; Aerden, 2004; Aerden *et al.*, 2010), analytical solutions (Jeffery, 1922; Ghosh and Ramberg, 1976; Jiang and Williams, 2004), or analogue and numerical modelling (Bjørnerud, 1989; Ildefonse *et al.*, 1992; Passchier *et al.*, 1993; Ceriani *et al.*, 2003; Griera, 2005). But so far there has been limited attention to the role of planar anisotropies in the deformation behaviour of rigid inclusions (Dabrowski and Schmid, 2011; Griera *et al.*, 2013).

This work aims to compare strain localization and partitioning around rigid inclusions

RESUMEN

Este trabajo se centra en cómo la rotación de partículas rígidas está influenciada por la anisotropía planar previa del medio envolvente durante la deformación. Se llevaron a cabo tres experimentos en el Laboratorio de Deformación de la UAB utilizando el aparato BCN-Stage. Los modelos se realizaron con material analógico (plastilina para la matriz y parafina para las inclusiones rígidas), siendo deformados por cizalla pura a tasa de deformación y temperatura constantes. Todas las inclusiones eran inicialmente idénticas en orientación y dimensión. En el primer experimento, cuya matriz consistió en plastilina homogénea, la rotación de las partículas rígidas se produjo de acuerdo con la prevista por los modelos teóricos. En los otros dos experimentos, las partículas rígidas se encontraban inmersas en un sistema multicapa de plastilina sometido a plegamiento. Las capas en ambos experimentos tenían vergencias inicialmente opuestas con respecto a los ejes cinemáticos. En estos dos casos, las inclusiones rígidas giran antitéticamente con respecto a las capas en plegamiento, independientemente de su orientación, lo cual indica la fuerte influencia de la anisotropía de las capas y su orientación en la rotación de los cuerpos. Los resultados se pueden correlacionar con ejemplos de campo

Palabras clave: Modelización analógica, partición de la deformación, plegamiento, multicapa, rotación de partículas rígida

Recepción: 26 de enero de 2016
Revisión: 20 de abril de 2016
Aceptación: 20 de Mayo de 2016

in homogeneous isotropic versus in layered anisotropic media, and to explore the influence of the orientation of the layer-induced anisotropy on the developed structures. This has been done by means of analogue modelling, and the results have been compared with previous field studies in the Culip area (Cap de Creus massif, Eastern Pyrenees).

Experimental procedure

Three experiments (named Exp. #1, #2 and #3) were performed using the deforma-

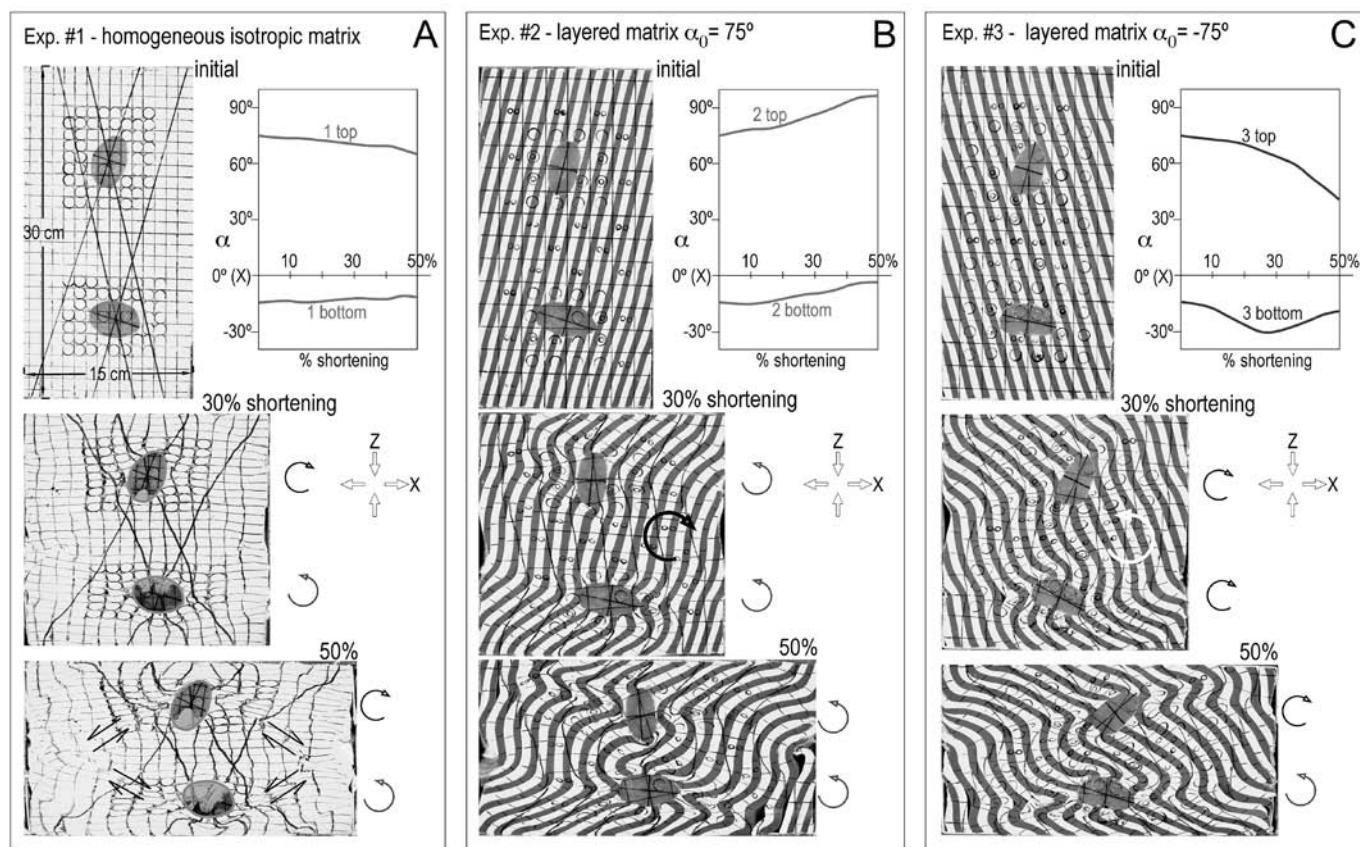


Fig. 1.- Sequential photographs of the three performed experiments (at initial stage, 30% and 50% bulk shortening) and diagrams showing the rotation of the rigid inclusions (angle α) with bulk shortening. Curved arrows indicate sense of rotation. A) Exp- #1. B) Exp- #2. C) Exp- #3.

Fig. 1.- Secuencia de fotografías de los tres experimentos realizados (en el estadio inicial, al 30% y al 50% de acortamiento global) y diagramas mostrando la rotación de las inclusiones rígidas (ángulo α) con el acortamiento global. Las flechas arqueadas muestran el sentido de rotación. A) Exp- #1. B) Exp- #2. C) Exp- #3.

tion device BCN-stage at the Universitat Autònoma de Barcelona (Druguet and Carreras, 2006).

The analogue materials used for the experiments are: (1) White and purple (dark grey in the images) plasticines from Ocluplast S.A., with an effective viscosity $\sim 10^7$ Pa.s., simulating the ductile host rock; (2) Vaseline Ricinol V from Brugarolas S.A., mixed with white plasticine in a 10%/90% volume proportion to obtain a low competence plasticine-vaseline mixture; and (3) Paraffin wax (melting temperature 56-58 °C by Panreac Química S.A.) as analogue for the rigid or close-to-rigid inclusions.

The models had the shape of rectangular boxes of initial dimensions 30x15x10 cm (Fig. 1). Pairs of elongated cylindrical cavities were filled with molten paraffin and left aside to completely solidify before the start of the experiments. The inclusions had an elliptical section of aspect ratio $\approx 2:1$, with the long axis at $\alpha_0 = 75^\circ$ (upper inclusion) and at $\alpha_0 = -15^\circ$ (lower inclusion) to the maximum extension direction (X). Linear passive markers were drawn as a 1x1 cm

grid on the upper surface of the models and, for Exp. #1 lines at $\pm 75^\circ$ to X were also drawn.

The three models were deformed with the prototype BCN-Stage by bulk pure shear (shortening along Z axis and extending along X axis; Fig. 1) at constant bulk strain rate ($2.5 \times 10^{-5} \text{ s}^{-1}$) and temperature (28 °C). Under these conditions, the effective viscosity contrast between more competent (dark plasticine) and less competent (white plasticine/vaseline mixture) is < 10 , whereas the effective viscosity of the paraffin bodies is at least two orders of magnitude higher than that of the plasticines (Castaño, 2010). A $\sim 50\%$ bulk shortening was attained in the three experiments.

The matrix of Exp. #1 consisted of a block of homogeneous white plasticine/vaseline mixture. In the cases of Exp. #2 and #3, the blocks consisted of multilayers of alternating layers of white plasticine/vaseline mixture and layers of purple plasticine, initially oriented along the shortening strain field. The only differing variable in Exp. #2 and #3 was the initial sense of layer trend with respect to the

maximum extension direction (X), represented as the angle α_0 ($\alpha_0 = 75^\circ$ in Exp. #2 and $\alpha_0 = -75^\circ$ in Exp. #3, Figs. 1B and 1C, respectively).

Results

Experiment #1

In this experiment with a rheologically homogeneous plasticine matrix, paraffin rigid inclusions rotate in a sense consistent with the theoretical pattern predicted for homogeneous pure shear. That is, both inclusions rotate into parallelism with the principal extension direction (X), the upper inclusion rotating in a clockwise sense and the lower one in an anti-clockwise sense (Fig. 1A). However, the rate at which inclusions rotate and the total amount of rotation are lower than the rate and amount of rotation of the bulk system. This is because deformation is partly accommodated by the plasticine matrix through the development of a conjugate system of localized dextral and sinistral shear zones surrounding the

rigid particles. This becomes evident by the linear passive markers.

Experiment #2

In this experiment with a multilayered matrix oriented at $\alpha_0 = 75^\circ$, rotation of the rigid particles does not follow the theoretical predictions for pure shear deformation. The layering in the matrix becomes folded while rotates towards X in a clockwise sense. This flexural flow process induces a sinistral layer-parallel shearing which is antithetic to the bulk layer rotation. In this case, the rigid inclusions rotate in an anti-clockwise sense coupled with the sinistral layer-parallel shearing (Fig. 1B).

Folds in the matrix are rather regular and asymmetric except around the contact with the inclusions. There, folds develop disharmonic shapes due to the antithetic rotation of the inclusions opposite to bulk layer rotation.

Experiment #3

In this case, the multilayered sequence was initially oriented at $\alpha_0 = -75^\circ$, oppo-

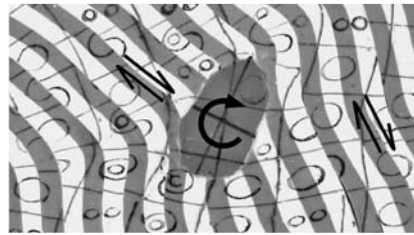


Fig. 2.- Detail of deformation partitioning around the upper paraffin particle of Exp. #3 at 30% bulk shortening.

Fig. 2.- Detalle mostrando la partición de la deformación alrededor de la particular superior de parafina del Exp. #3 para un 30% de acortamiento global.

site to the symmetry of Exp. #2. The rotational behaviour of the rigid particles is again controlled by the flexural flow in the matrix. In this case, both rigid particles rotate in a clockwise sense coupled with the dextral layer-parallel shearing (Figs. 1C and 2). However, after ~30% bulk shortening, the sense of rotation of the lower inclusion is reversed from clockwise to anti-clockwise (Fig. 1C). Such a reversal in rotation sense is coeval with the local reversal of the rotation sense of the layering (anti-

clockwise to clockwise) in the short limbs of the folds.

The inclusions in Exp. #3 experienced the highest rotation rate, followed by those in Exp. #2 and Exp. #1 (compare the slopes of the curves in the diagrams of Fig. 1).

Comparison with field structures

The results obtained from these experiments can be compared with field structures involving complex and differential deformation behaviour of rigid or competent particles (porphyroblasts/clasts, boudins, or even large plutons) with respect to an anisotropic surrounding media.

For instance, Variscan deformation in the Culip area (NE Cap de Creus) is interpreted as a situation that bears many analogies with the experiments presented here. In a sequence of layered and foliated metasedimentary rocks, all kinematic indicators are apparently contrary to the hectometric dextral deflection of layering (Fig. 3). It was shown in previous studies (Carreras and Druguet, 1994; Druguet *et al.*, 1997; Carreras *et al.*, 2013) that the bulk dextral deflec-

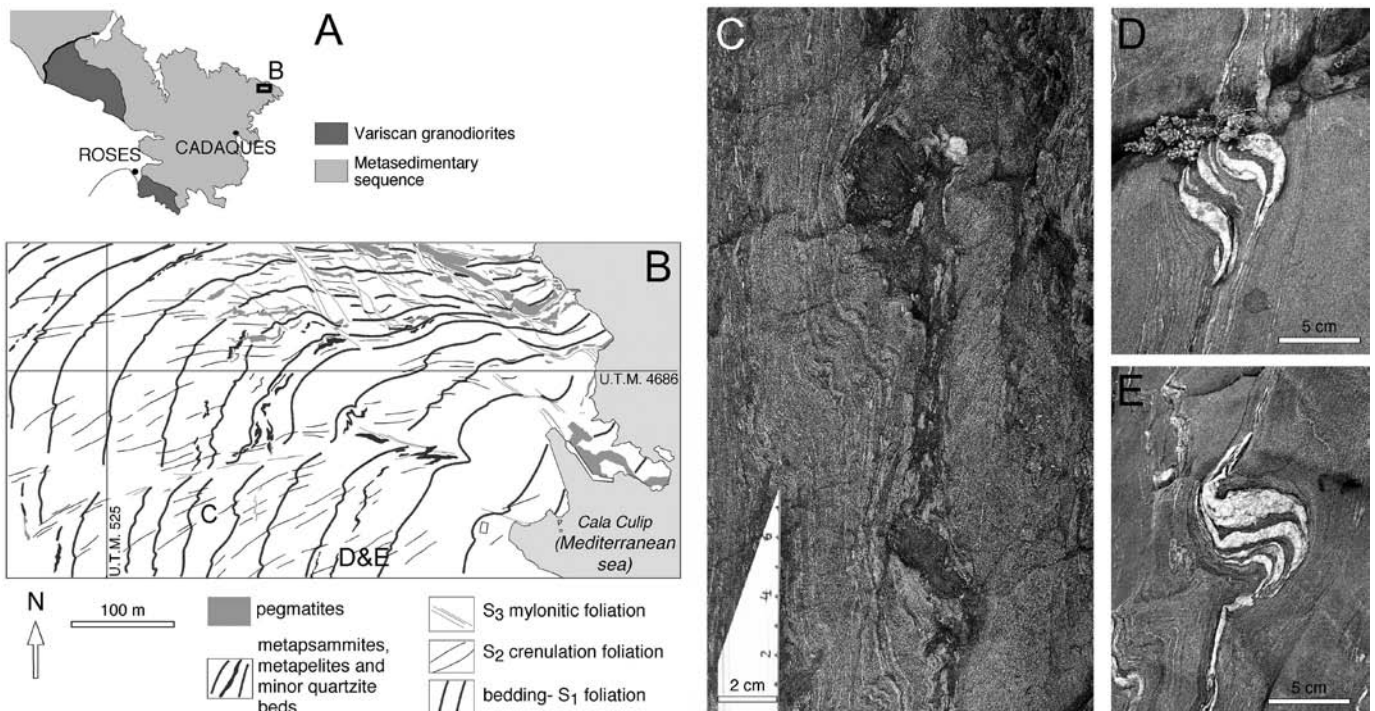


Fig. 3.- Example of a complex strain partitioning pattern in the Culip area (Cap de Creus massif). A) Geological sketch of the Cap de Creus massif. B) Structural sketch of part of the Culip area (modified from Carreras and Druguet, 1994). Coordinate system UTM 31N ED50. C) Porphyroblasts of andalusite showing anti-clockwise rotation with respect to the enveloping schistose banding. D) and E) Two examples of quartz rods showing different degrees of anti-clockwise rotation.

Fig. 3.- Ejemplo de un patron complejo de partición de la deformación en el área de Culip (Cap de Creus). A) Esquema geológico del macizo de Cap de Creus. B) Esquema estructural de una parte del área de Culip (modificado de Carreras y Druguet, 1994). Sistema de coordenadas UTM 31N ED50. C) Porfiroblastos de andalucita mostrando rotación antihoraria en relación al bandeado esquistoso. D) y E) Dos ejemplos de "rods" de cuarzo mostrando rotación antihoraria en diferente grado.

tion structure is accommodated by flexural flow, producing the anti-clockwise rotation of competent bodies such as porphyroblasts and rod-shaped quartz veins (Fig. 3C, D and E). More exactly, dextral transpression (which includes a coaxial component as in the experiments) is partitioned into asymmetric folding of the layers, sinistral layer-parallel shear and vertical extension.

Conclusions

The rheological and mechanical properties of the matrix materials play a determinant role in deformation partitioning. The presence of a layer anisotropy and its relative orientation with respect to the kinematic framework and to the orientation of the particles is determinant in the resulting structures and the sense of rotation of rigid bodies.

Despite the limitations involved in these relatively simple analogue models, all the results can be consistently interpreted. In case of an homogeneous isotropic matrix, the rotation sense of rigid particles is governed by their angular relationships with regard to the bulk kinematic framework (pure shear in our experiments).

In the second and third models, in which the matrix was a multilayer, rotation of rigid inclusions is mainly controlled by the relative orientation of the layering and the kinematic axes. Rigid inclusions tend to rotate antithetically with respect to the layers that are being folded, regardless of the orientation of the inclusions with respect to the bulk strain axes, a fact that has not been observed in numerical simulations under simple shear (e.g. Griera *et al.*, 2013). Thus, it seems

that the rotation behaviour of rigid particles can be especially complex in deformation regimes involving a coaxial component.

These results have important implications and must be taken into account for the tectonic interpretation of deformed layered or foliated rocks.

Acknowledgements

We gratefully acknowledge helpful suggestions by the editor Carlos Liesa and careful reviews by Domingo Aerden and Manuel Díaz Azpiroz.

References

- Aerden, D.G.A.M. (2004). *Journal of Structural Geology* 26, 177-196.
- Aerden, D.G.A.M., Sayab, M. and Bouybaouene, M.L. (2010). *Journal of Structural Geology* 32, 1030-1045.
- Bell, T.H. (1985). *Journal of Metamorphic Geology* 3, 109-118.
- Bjørnerud, M. (1989). *Journal of Structural Geology* 11, 245-254.
- Carreras, J. and Druguet, E. (1994). *Journal of Structural Geology* 16, 1525-1534.
- Carreras, J., Cosgrove, J. and Druguet, E. (2013). *Journal of Structural Geology* 50, 7-21.
- Castaño, L.M. (2010). *Emplazamiento y deformación de venas y diques magmáticos en cinturones tectonometamórficos: Análisis a partir de estudios de campo y modelización analógica*. Tesis Doctoral, Univ. Autònoma de Barcelona, 275 p.
- Ceriani, S., Mancktelow, N.S. and Pennacchioni, G. (2003). *Journal of Structural Geology* 25, 2005-2021.
- Dabrowski, M. and Schmid, D.W. (2011). *Journal of Structural Geology* 33, 1169-1177.
- Druguet, E. and Carreras, J. (2006). *Journal of Structural Geology* 28, 1734-1747.
- Druguet, E., Passchier, C.W., Carreras, J., Victor, P. and den Brok, S.W.J. (1997). *Tectonophysics* 280, 31-45.
- Ghosh, S.K. and Ramberg, H. (1976). *Tectonophysics* 34, 1-70.
- Griera, A. (2005). *Estructures tectòniques i la seva relació amb la vorticitat cinemàtica: Casos reals i models*. Tesis Doctoral, Univ. Autònoma de Barcelona, 582 p.
- Griera, A., Llorens, M.-G., Gomez-Rivas, E., Bons, P.D., Jessell, M.W., Evans, L.A. and Lebensohn, R. (2013). *Tectonophysics* 587, 4-29.
- Ildefonse, B., Launeau, P., Bouchez, J.L. and Fernandez, A. (1992). *Journal of Structural Geology* 14, 73-83.
- Jeffery, G.B. (1922). In: *Proceedings of the Royal Society of London Series A* 102, 161-179.
- Jiang, D. and Williams, P.F. (2004). *Journal of Structural Geology* 26, 221-2224.
- Johnson, S.E. (1999). *American Mineralogist* 84, 1711-1726.
- Passchier, C.W. and Simpson, C. (1986). *Journal of Structural Geology* 8, 831-843.
- Passchier, C.W. and Trouw, R.A.J. (2005). *Microtectonics*. Springer Verlag, 2nd edition, Berlin. 366 p.
- Passchier, C.W., ten Brink, C.E., Bons, P.D. and Sokoutis, D. (1993). *Earth and Planetary Science Letters* 120, 239-245.
- Schoneveld, C. (1977). *Tectonophysics* 39, 453-471.
- Vernon, R.H. (1978). *Geologische Rundschau* 67, 288-305.